

Theoretical Research on a Multibeam-Modulated Electron Gun Based on Carbon Nanotube Cold Cathodes

Xuesong Yuan, Bin Wang, Matthew T. Cole, Yu Zhang, Shaozhi Deng, William I. Milne, and Yang Yan

Abstract—Multi-beam modulation in a carbon nanotube (CNT) cold cathode electron gun is herein investigated in order to develop miniaturized and fully integrated vacuum electron devices. By exposing the electron source to a millimeter-wave signal, the steady-state field emission current density is efficiently modulated by the incident high-frequency (HF) electric field. Our simulation results of this multibeam electron gun show that the field emission current density can be efficiently modulated by different incident frequency millimeter waves. We find that the modulation depth is increased by enhancing the HF input power and anode operation voltage. The modulation frequency and phase of each electron beam can be controlled using a single millimeter-wave source and by simply adjusting the lateral distance between adjacent CNT cold cathodes.

Index Terms—Carbon nanotube (CNT), cold cathode, electron gun, multibeam.

I. INTRODUCTION

DUE to their high-power and high-frequency (HF) operation, vacuum electron radiation sources underpin radar, communication, and particle accelerator systems [1]. Nevertheless, large working volumes, high-temperature operation, and slow reaction times, due to the need for thermionic cathodes, have limited the application of vacuum electron radiation sources in some fields. Solid-state electron radiation sources have attracted increasing attention of late. They have developed rapidly and have replaced their vacuum counterparts in many applications. Their simple miniaturization, low working voltages, room-temperature operation, and ready integration are particularly attractive. However, solid-state electron radiation sources have some limitations; their poor

anti-interference performance, deleterious responsiveness to incident radiation, and low output power in the millimeter-wave and terahertz frequency bands are perhaps some of the most critical issues plaguing solid-state radiation sources to date. Vacuum microelectronic (VME) devices combine vacuum and solid-state electronics [2]. They have many advantages inherited from both the vacuum and solid-state electron devices upon which they are based, including HF operation, low-temperature operation, and simple integration. Central to such VME radiation sources is the derivation of a room-temperature, rapidly time-responding electron beam based on field emission cold cathode sources. Carbon nanotubes (CNTs) have proved to be a leading field emission material [3]. Such nanoengineered devices mediate high emission current densities, impressive chemical stability, mechanical strength, and temporal stability [4], making CNTs well suited to underpin the next generation of VME radiation sources [5]–[9].

To develop integrated VME radiation sources, there are two key technologies requiring consideration. The first of these is the effective beam–wave interaction. VME devices are often small in volume (typically less than 1 cm³) while the electron beam velocity is near relativistic. In such a regime, the limited interaction time makes it challenging to impart high energy densities from the HF field to the emerging modulated electron beam. Traditional vacuum electron devices have shown that if the HF field interacts with a prior-modulated electron beam, the beam–wave interaction efficiency will be improved somewhat as a result [10]–[12]. Therefore, it is very important to develop means of modulating the source electron beam prior to HF field exposure. Second, frequency and phase synchronization of each radiation source is evidently a key challenge to be resolved. Different frequency radiation sources are often difficult to integrate within single package. For phase-unsynchronized same-frequency radiation sources, phase-coherency problems often arise, which dramatically reduce the functionality of the integrated VME radiation sources.

In this paper, we develop a multibeam-modulated CNT cold cathode electron gun toward realizing a fully integrated VME radiation source. First, a modulation method is proposed based on conventional field emission theory [13], [14]. In this first instance, the field emission beam is wholly modulated by the HF field confined within the cavity. We find that the power of electron beam is low and the modulation phase of different emerging beams lacks control. In this method,

Manuscript received March 4, 2016; revised April 19, 2016 and May 5, 2016; accepted May 6, 2016. This work was supported in part by the National Basic Research Program of China under Grant 2013CB933603 and in part by the National Natural Science Foundation of China under Grant U1134006 and Grant 61101041. The review of this paper was arranged by Editor M. Thumm.

X. Yuan, B. Wang, and Y. Yan are with the School of Physical Electronics, University of Electronic Science and Technology of China, Chengdu 610054, China (e-mail: yuanxs@uestc.edu.cn; wb@uestc.edu.cn; yanyang@uestc.edu.cn).

M. T. Cole and W. I. Milne are with the Electrical Engineering Division, Department of Engineering, University of Cambridge, Cambridge CB3 0FA, U.K. (e-mail: mtc35@cam.ac.uk; wim@eng.cam.ac.uk).

Y. Zhang and S. Deng are with the State Key Laboratory Optoelectronic Materials and Technologies, Sun Yat-sen University, Guangzhou 510275, China (e-mail: stszhyu@mail.sysu.edu.cn; stsdz@mail.sysu.edu.cn).

Color versions of one or more of the figures in this paper are available online at <http://ieeexplore.ieee.org>.

Digital Object Identifier 10.1109/TED.2016.2565583

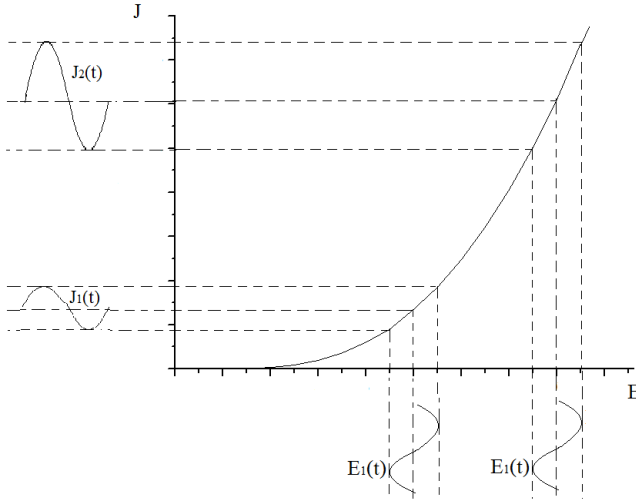


Fig. 1. Field emission beam current density as a function of electric field during dc-shifted ac excitation.

both the electrostatic field and HF field act concurrently on the CNT cold cathode. A modulated electron beam is generated even when the millimeter-wave input power is very weak (<1 W). The electron beam power can be significantly improved by increasing anode operation voltage (>1 W/100 V). In the second part of this paper, we show how the entire electron beam can be modulated by the same HF field, thereby allowing for the modulation frequency and phase of each electron beam to be controlled to solve the above-mentioned integration problem, allowing us to realize novel VME radiation sources.

II. MODULATION THEORY

The field emission current density (J) is given by simplified Fowler–Nordheim equation of the form

$$J = AE^2 \exp\left(-\frac{B}{E}\right) \quad (1)$$

where E is the local electric field, and A and B are the approximate Fowler–Nordheim constants. The electric field includes a varying time-domain component: $E(t) = E_0 + E_1(t)$. Here E_0 is the direct current (dc) electrostatic field, $E_1(t)$ is the HF field, and $|E_1(t)| \ll |E_0|$. Equation (1) now gives

$$\begin{aligned} J(t) &= AE^2(t) \exp\left[-\frac{B}{E(t)}\right] \\ &= A[E_0 + E_1(t)]^2 \exp\left[-\frac{B}{E_0 + E_1(t)}\right] \\ &= \dots = J_0 + J_1(t). \end{aligned} \quad (2)$$

Based on (2), we find that the field emission beam current density is composed of two terms; one is the dc component (J_0) and the other is the alternating current (ac) component (J_1). Fig. 1 shows the field emission beam current density as a function of electric field in the unlimited emission regime. With the superposition of an HF field $E_1(t)$, a time-modulated current density $J_1(t)$ is obtained. For an increased E_0 , and maintained source $E_1(t)$, different resulting J_1 and J_2

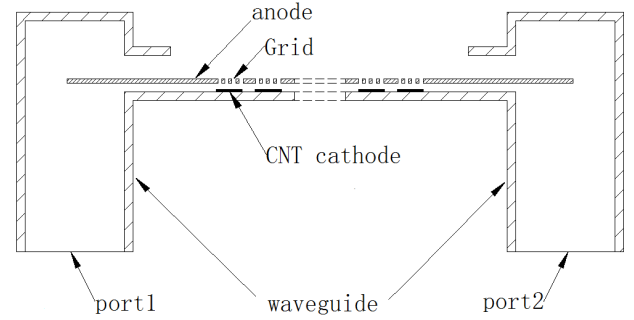


Fig. 2. Scheme of modulated multibeam CNT cold cathode electron gun.

ac components, and hence modulation depths, are obtained. When the electrostatic field is larger, the ac current density component is greater. The magnitude of the dc source amplifies the ac output.

III. MULTIBEAM MODULATION ELECTRON GUN

In this section, a high-modulation-efficiency CNT cold cathode electron gun is investigated using a 3-D electromagnetic simulation software computer simulation technology (CST) STUDIO SUITE. The proposed device includes an HF field input and output structure which acts on the CNT electron sources. In the latter part of this section, the modulation of a single electron gun is simulated. Finally, the modulation frequency and phase control of differing beams is considered in this CNT cold cathode electron gun structure by CST.

A. Modulating HF CNT Electron Gun Device Geometry

In order to obtain high efficiency modulation, the direction of the HF electric field should align with the electrostatic field vector. In the present device, we have selected a parallel plate geometry, denoted by anode and cathode in Fig. 2, which is similar to that of a traditional microstripline. The conducting strip (upper plate) is the perforated anode and the CNT is located on the lower plate, which is the cathode. Both the electrostatic and HF fields lie perpendicular to the anode–cathode structure. The HF field is transmitted in the parallel plate structure with a transverse electromagnetic (TEM) mode.

Fig. 2 depicts the modulated multibeam CNT cold cathode electron gun scheme. The HF field is transmitted into the interelectrode gap from port1 of the rectangular waveguide. The TE_{10} mode of the HF field in the rectangular waveguide is converted to a TEM mode within the parallel plate structure and subsequently passes the linear array of CNT cold cathodes. The HF field exits from port2 on the right side of the waveguide. The lower plate is connected to the waveguide upon which the CNT cathodes are fixed. When the electron gun operates, the anode is set at high dc potential, resulting in a time-stable field emission dc. An HF field is then introduced propagating along the waveguide and interacting with the CNT cold cathodes within the TEM mode of the interelectrode gap. The time-stable electron beams are thusly modulated. Through grid holes in the anode, modulated electron beams are emitted.

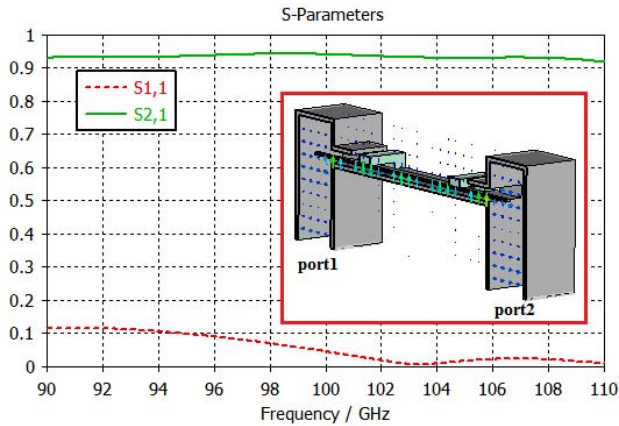


Fig. 3. S_{11} and S_{21} parameters of the HF modulation structure. Inset: HF electric field vector across the source waveguide cross section.

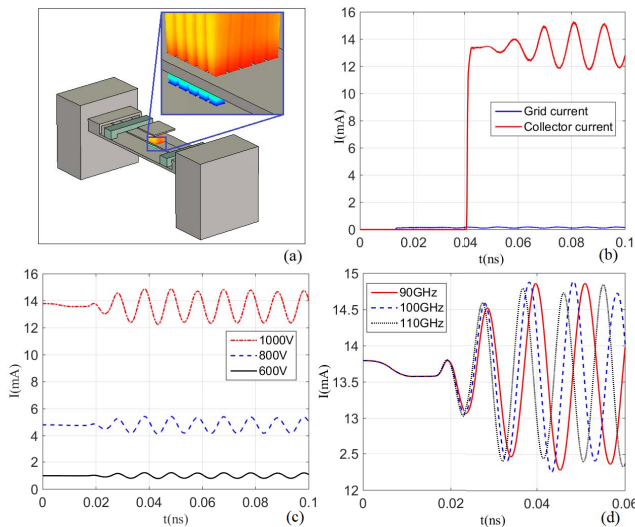


Fig. 4. CNT cathode single-beam modulation. (a) Structure of the electron gun. Inset: resulting electron trajectories. (b) Grid current and collector current. (c) Modulated beam current as a function of dc operation voltage. (d) Beam current amplitude modulation as a function of HF field ($P_{in} = 5$ W, $U_0 = 1000$ V).

To ensure minimal leakage, the anode's laser-cut grid holes are smaller than the wavelength of the HF field.

Fig. 3 shows, for perturbations about a nominal 3-mm (100-GHz) HF field, the simulated S -parameters and electric field vector across the source cross section. Here the input and output waveguides are WR_{10} ($a \times b = 2.54 \times 1.27$ mm), which is modeled as lossy copper. The width of the lossy steel anode is 0.5 mm. The anode is fixed to the cathode by two dielectric brackets. The distance between the anode and cathode is 0.1 mm. Our simulation results show that the HF field transmits well in the range of 90–110 GHz via the TEM mode in the interelectrode gap, with a maximum insertion loss of about -0.7 dB.

B. Single-Beam-Modulated Electron Gun

In this section, a single-beam-modulated electron gun is further studied in the range of 90–110 GHz. Fig. 4(a) shows

the structure of the electron gun and the resultant electron trajectories. The gun consists of an array of 5×5 CNT cold cathodes, each unit being 0.05×0.05 mm². The height of the CNTs is 3 μ m. The distance between adjacent unit centers is 0.075 mm. To ensure a high anode electron transparency, an array of 5×5 apertures is integrated into the anode. The aperture geometry is congruent with the CNT unit layout, except for each unit being 0.06×0.06 mm. In our CNT field emission simulations, we employ the experimental model, as in [15]. Based on (1), A and B can be obtained by numerical fitting based on our earlier experimental results [16], [17]. We find experimentally that $A = 2.8 \times 10^{-8}$ A/V² and $B = 2.29 \times 10^7$ V/m. The input power from the HF field is 5 W. Simulation results show that anode grid beam transparency is up to 99%, as shown in Fig. 4(b). We find that the modulation depth of the collector current (11.7–15.2 mA) in Fig. 4(b) is larger than the emission current at an operational voltage of 1000 V (12.3–14.8 mA) [Fig. 4(c)]. We attribute this to the fact that the emitted electrons are simultaneously accelerated by the HF and electrostatic fields, though there nevertheless remains a certain population which presents a varied velocity range. If the size of aperture is increased, the beam transparency of the grid will reach 100%. However, this is at the expense of the surface electric field, which will become increasingly weak for increasing aperture diameter. The electric field incident at the center of the cathode surface will, in the present optimal geometry, be reduced by some 46%. Such field reduction is common to gated field emission cold cathodes. To counteract this reduction at the cathode center, we are investigating different CNT bundle geometries in order to mediate high enhancement factors [18].

Fig. 4(c) shows the electron beam modulated by a 100-GHz HF field under different dc operation voltages. For dc operation voltages (U_0) of 600, 800, and 1000 V, the electron beam currents, I_0 , are 0.97, 4.79, and 13.58 mA, respectively (for $0 < t \leq 0.02$ ns). For $t \leq 0.02$ ns, as the HF field has not as yet reached the CNT cathodes, the dc beam current remains largely unchanged and time invariant. For $t > 0.02$ ns, the HF field begins to modulate the electron beam and the resulting amplitude modulation (under different dc operation voltages) is given by $\Delta I = (I_{max} - I_{min})/2$ and is 0.2, 0.6, and 1.25 mA, respectively. The modulation currents are increased with increasing dc operation voltage. Further simulations show that if we increase the HF input power, the modulation current also increases. Fig. 4(d) illustrates how the electron beam is modulated by different HF frequencies. For a single CNT cathode, we note that the amplitude modulation for different-frequency HF fields is almost invariant with HF under standard operating conditions ($P_{in} = 5$ W, $U_0 = 1000$ V).

C. Modulation Frequency and Phase Control in a Multibeam Electron Gun

In this section, the distribution of the HF field within the multibeam electron gun is analyzed. We then consider means of regulating the modulation frequency and phase control of the multibeam system. Herein we investigate a nominal

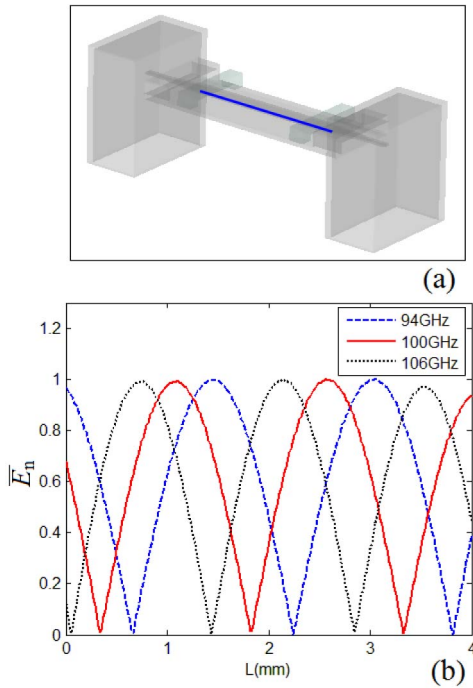


Fig. 5. (a) Structure of the multibeam HF-modulated source. (b) Absolute normalized HF electric fields along indicated blue cross section as in Fig. 5(a).

five-beam system, where all the beams are in phase with each other, and all of which operate at a single frequency.

Fig. 5(a) shows the structure of the multibeam HF-modulated source. The absolute value of the normalized HF electric field \bar{E}_n , aligned parallel to the direction of propagation, is shown in Fig. 5(b). Three principal frequencies are considered: 94, 100, and 106 GHz. The half-wavelength of the HF field along the transmission direction, $L_{\lambda/2}$, for the three frequency regimes considered, is $L_{\lambda/2}^{94} = 1.57$ mm, $L_{\lambda/2}^{100} = 1.49$ mm, $L_{\lambda/2}^{106} = 1.41$ mm. Based on $L_{\lambda/2}$, we set the distance between two adjacent CNT cathodes, allowing geometric control over the beam modulation depth due to engineered intrabeam interference. When the distance between two CNT cathodes is equal to $(2n + 1)L_{\lambda/2}$, $n = 1, 2, 3 \dots$, the modulation phase is equal and opposite. When the distance between two adjacent CNT cathodes is equal to $2nL_{\lambda/2}$, $n = 1, 2, 3 \dots$, the modulation phase is equal for all the emitters. As $L_{\lambda/2}$ is frequency dependent and there are multiple beams along the direction of propagation of HF fields, the phase difference between various modulation frequencies will manifest if we set the source to operate at a fixed mid-frequency of 100 GHz with $L_{\lambda/2}^{100} = 1.49$ mm. Considering this case, if the phase compensation for different frequencies cannot be achieved, we ultimately limit the modulation frequency range and the number of electron beams (and hence the total output power).

In the five-beam electron gun system, the size of each CNT cathode is about 0.4 mm. As a result we have physically limited the maximum distance between different frequency bands to $D_{\max} = 5 \times |L_{\lambda/2}^{f_1} - L_{\lambda/2}^{f_2}|$, which should be < 0.4 mm, where f_1 denotes the mid-frequency and f_2 is

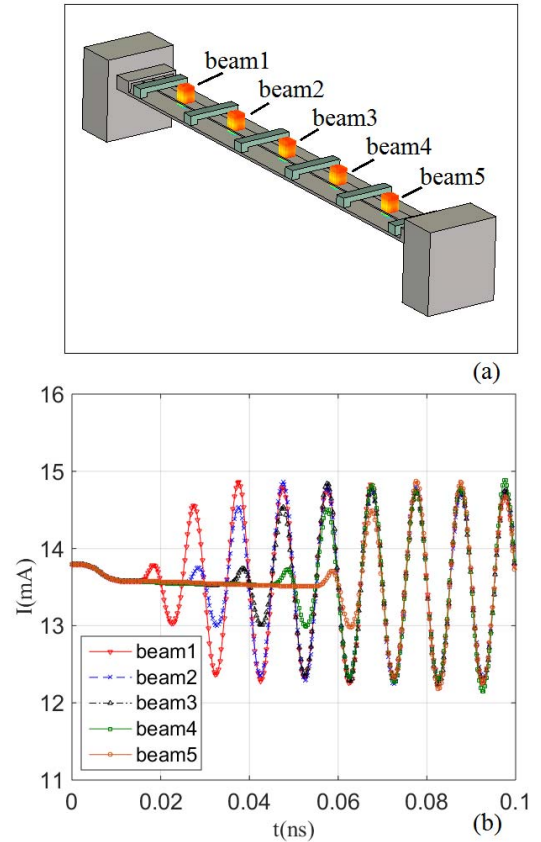


Fig. 6. Five-beam-modulated CNT cold cathode electron gun. (a) Scheme depicting the electron gun structure and resulting electron trajectories. (b) Electron beam currents from each of the five electron sources, as a function of time, for a modulation frequency of 100 GHz.

the minimum/maximum frequency. When the modulation mid-frequency is 100 GHz, the modulation frequency range is from 94 to 106 GHz. Here the distance between two adjacent CNT cathodes is 2.98 mm. Fig. 6(a) shows the structure of the electron gun and the five electron beam trajectories under these operating conditions. Each electron beam is generated from a 5×5 CNT array, where all other geometric parameters are the same as those in the earlier single-beam modulation system. Fig. 6(b) shows the beam current for the five electron beams, as a function of time, for a modulation frequency of 100 GHz. Initially, the five electron beam currents are all 13.58 mA as there is no HF field. When $t = 0.015$ ns, the first beam is modulated; when $t = 0.025$ ns, the second beam is modulated, where the modulation phase of the second beam is equal to that of the first beam. The following three beams are subsequently modulated successively. When $t = 0.07$ ns, the modulation of the five beams achieves a steady-state condition, with all five beams being in phase.

To realize broadband frequency modulation, the 94- and 106-GHz cases have been simulated in the five-beam CNT cold cathode electron gun. Fig. 7(a) shows the beam currents for the five electron beams modulated at an HF field of 94 GHz. Note that the modulation sequence of the five beams is the same as that of the 100-GHz case and that the five-beam modulation frequency is also equivalent. If the phase of beam 3 is set as the center phase. The phase

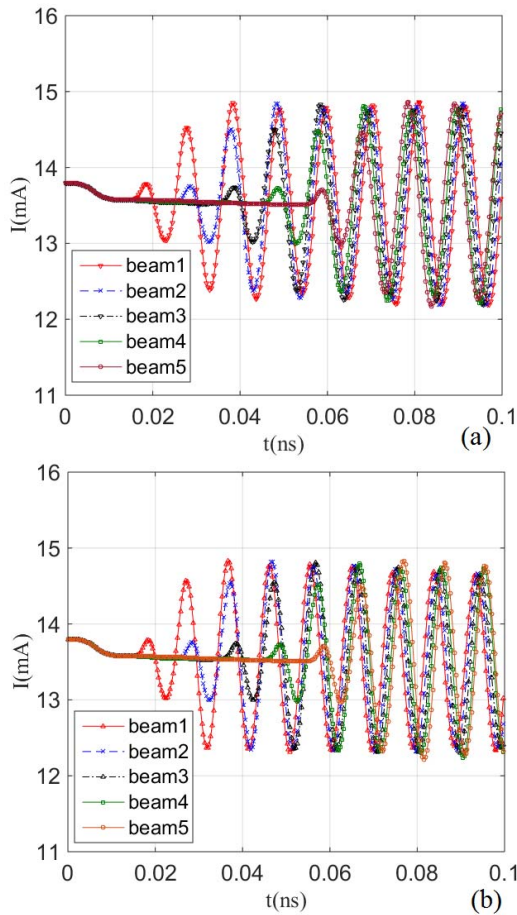


Fig. 7. Broadband modulation of the five-beam CNT cold cathode electron gun. Five-beam current variation with time for (a) 94 GHz and (b) 106 GHz HF fields.

between beams 3 and 1 or between beams 3 and 5 has only a very slight difference ($< \pm 0.05\pi$), which our studies show is largely negligible as it pertains to the device operation. Fig. 7(b) shows five electron beams modulated by a 106-GHz HF field. As $L_{\lambda/2}^{106}$ is smaller, the phase difference for beams 3 and 1 or beams 3 and 5 is larger than that for 94-GHz modulation. Nevertheless, it remains comparatively small ($< \pm 0.06\pi$). Further simulations have shown that the phase difference of two beams tends to decrease as the modulation frequency tends to 100 GHz. We can therefore, in the present device geometry, effectively adjust the modulation frequency range according to the functional requirements of vacuum devices.

IV. CONCLUSION

Here we have studied the HF modulation of the dc field emission current density from CNT-based cold cathode radiation sources in order to develop miniaturized and highly integrated vacuum electron devices. The studied geometry allows for an increased modulation depth by increasing the HF field input power in addition to the driving electrostatic field. By controlling both the HF field and electrostatic field, we have demonstrated a viable means of high-power electron beam modulation. The modulated electron beam can be used

not only to interact with the output-modulated HF field, realized millimeter-wave amplification, but also to stimulate terahertz oscillator via frequency multiplication in a resonant cavity.

A methodology to control the modulation frequency and phase in a linear multibeam CNT field emission electron gun has been outlined. The detailed modulated electron beams allow stimulation of different millimeter-wave/terahertz radiation sources, the frequency and phase of which will be locked, thereby allowing for fully integrated vacuum radiation sources. Broadband modulation and amplification have been realized, which offer a means to develop next-generation communication amplifiers based on emerging nanocarbon materials.

REFERENCES

- [1] R. J. Barker and E. Schamiloglu, *High-Power Microwave Sources and Technologies*. New York, NY, USA: Wiley, 2001.
- [2] W. Zhu, *Vacuum Microelectronics*. New York, NY, USA: Wiley, 2001.
- [3] C. M. Collins, R. J. Parmee, W. I. Milne, and M. T. Cole, "High performance field emitters," *Adv. Sci.*, vol. 1500318, pp. 1–8, Feb. 2016.
- [4] R. H. Baughman, A. A. Zakhidov, and W. A. de Heer, "Carbon nanotubes—The route toward applications," *Science*, vol. 297, no. 5582, pp. 787–792, 2002.
- [5] F. Brunetti *et al.*, "Flip-cathode design for carbon nanotube-based vacuum triodes," *IEEE Electron Device Lett.*, vol. 29, no. 1, pp. 111–113, Jan. 2008.
- [6] G. Ulisse *et al.*, "Carbon nanotube cathodes for electron gun," *IEEE Electron Device Lett.*, vol. 34, no. 5, pp. 698–700, May 2013.
- [7] G. Ulisse, F. Brunetti, and A. Di Carlo, "Study of the influence of transverse velocity on the design of cold cathode-based electron guns for terahertz devices," *IEEE Trans. Electron Devices*, vol. 58, no. 9, pp. 3200–3204, Sep. 2011.
- [8] H. M. Manohara, R. Toda, R. H. Lin, A. Liao, M. J. Bronikowski, and P. H. Siegel, "Carbon nanotube bundle array cold cathodes for THz vacuum tube sources," *J. Infr., Millim., Terahertz Waves*, vol. 30, pp. 1338–1350, Dec. 2009.
- [9] H. J. Kim, J. J. Choi, J.-H. Han, J. H. Park, and J.-B. Yoo, "Design and field emission test of carbon nanotube pasted cathodes for traveling-wave tube applications," *IEEE Trans. Electron Devices*, vol. 53, no. 11, pp. 2674–2680, Nov. 2006.
- [10] J. H. Booske *et al.*, "Vacuum electronic high power terahertz sources," *IEEE Trans. THz Sci. Technol.*, vol. 1, no. 1, pp. 54–75, Sep. 2011.
- [11] C. B. Wilsen, Y. Y. Lau, D. P. Chernin, and R. M. Gilgenbach, "A note on current modulation from nonlinear electron orbits," *IEEE Trans. Plasma Sci.*, vol. 30, no. 3, pp. 1176–1178, Jun. 2002.
- [12] S. A. Kitsanov *et al.*, "S-band vircator with electron beam premodulation based on compact pulse driver with inductive energy storage," *IEEE Trans. Plasma Sci.*, vol. 30, no. 3, pp. 1179–1185, Jun. 2002.
- [13] K. B. K. Teo *et al.*, "Microwave devices: Carbon nanotubes as cold cathodes," *Nature*, vol. 437, no. 7061, p. 968, Oct. 2005.
- [14] P. Legagneux *et al.*, "Carbon nanotube based cathodes for microwave amplifiers," in *Proc. IEEE Int. Vac. Electron. Conf.*, Apr. 2009, pp. 80–81.
- [15] C. Li *et al.*, "High emission current density, vertically aligned carbon nanotube mesh, field emitter array," *Appl. Phys. Lett.*, vol. 97, no. 11, p. 113107, 2010.
- [16] Y. Xue-Song *et al.*, "Study of pulsed field emission characteristics and simulation models of carbon nanotube cold cathodes," *Acta Phys. Sinica* vol. 61, no. 21, p. 216101, Nov. 2012.
- [17] X. Yuan *et al.*, "A gridded high-compression-ratio carbon nanotube cold cathode electron gun," *IEEE Electron Device Lett.*, vol. 36, no. 4, pp. 399–401, Apr. 2015.
- [18] M. T. Cole, K. B. K. Teo, O. Groening, L. Gangloff, P. Legagneux, and W. I. Milne, "Deterministic cold cathode electron emission from carbon nanofibre arrays," *Sci. Rep.*, vol. 4, no. 4840, May 2014.



Xuesong Yuan received the B.S. degree in physics from Anhui University, in 2002, and the Ph.D. degree in plasma physics from the University of Electronic Science and Technology of China (UESTC), in 2008.

He is currently an Associate Professor with UESTC. His current research interests include millimeter-wave and terahertz radiation generation, cold cathode particle beam generation and radiation sources.



Bin Wang received the B.S. and Ph.D. degrees in plasma physics from the University of Electronic Science and Technology of China, Chengdu, China, in 2002 and 2007, respectively.

He focuses on research of cold cathode millimeter-wave devices and high power microwave devices. He is a Lecturer with the University of Electronic Science and Technology of China.



Matthew T. Cole received the M.Eng. degree in engineering sciences from Oxford University, U.K., in 2008, and the Ph.D. degree in electrical engineering from Cambridge University, U.K., in 2011.

He is currently an Oppenheimer Research Fellow with the Department of Engineering, Cambridge University. His current research interests include the heterogeneous integration of chemical vapor deposited aligned nanomaterials.



Yu Zhang received the B.Sc. and Ph.D. degrees in physics from Sun Yat-sen University, Guangzhou, China, in 2003 and 2008, respectively.

He is currently an Associate Professor with Sun Yat-sen University.



Shaozhi Deng received the M.Sc. degree in electronics from the University of Electronic Science and Technology, Chengdu, China, in 1987, and the Ph.D. degree in physics from Sun Yat-sen University, Guangzhou, China, in 2010.

She is currently a Professor with Sun Yat-sen University.



William I. Milne received the B.Sc. degree from the University of St Andrews, U.K., in 1970, the Ph.D. degree in electronic materials and the D.I.C. degree from Imperial College London, U.K., in 1973.

He is currently Professor Emeritus in the Electrical Engineering Division, Department of Engineering, Cambridge University, and Visiting Professor at Zhejiang University, China.



Yang Yan received the B.S. and Ph.D. degrees from the University of Electronic Science and Technology of China (UESTC), in 1986 and 1995, respectively.

He is currently engaged in research with the Terahertz Researcher Center, UESTC, where he is involved in the areas of gyrotrons, laser fusion, free-electron lasers, high power microwaves, and fundamental plasma physics. He is a Professor with UESTC.